The negligible chondritic contribution in the lunar soils water

Alice Stephant[1] and François Robert

Institut de Minéralogie, de Physique des Matériaux, et de Cosmochimie, Sorbonne Universités, Muséum National d'Histoire Naturelle, Université Pierre et Marie Curie Paris 06, Unité Mixte de Recherche Centre National de la Recherche Scientifique 7590, Institut de Recherche pour le Développement Unité Mixte de Recherche 206, 75005 Paris, France

Edited by Mark H. Thiemens, University of California, San Diego, La Jolla, CA, and approved September 10, 2014 (received for review May 3, 2014)

Recent data from Apollo samples demonstrate the presence of water in the lunar interior and at the surface, challenging previous assumption that the Moon was free of water. However, the source(s) of this water remains enigmatic. The external flux of particles and solid materials that reach the surface of the airless Moon constitute a hydrogen (H) surface reservoir that can be converted to water (or OH) during proton implantation in rocks or remobilization during magmatic events. Our original goal was thus to quantify the relative contributions to this H surface reservoir. To this end, we report NanoSIMS measurements of D/H and ^{7}Li/^{6}Li ratios on agglutinates, volcanic glasses, and plagioclase grains from the Apollo sample collection. Clear correlations emerge between cosmogenic D and ^{6}Li revealing that almost all D is produced by spallation reactions both on the surface and in the interior of the grains. In grain interiors, no evidence of chondritic water has been found. This observation allows us to constrain the H isotopic ratio of hypothetical juvenile lunar water to $\delta D \leq -550‰$. On the grain surface, the hydroxyl concentrations are significant and the D/H ratios indicate that they originate from solar wind implantation. The scattering distribution of the data around the theoretical D vs. ^{6}Li spallation correlation is compatible with a chondritic contribution <15%. In conclusion, (*i*) solar wind implantation is the major mechanism responsible for hydroxyls on the lunar surface, and (*ii*) the postulated chondritic lunar water is not retained in the regolith.

hydrogen | lithium | moon | chondrites

Three types of sources could contribute to lunar superficial and mantle water, namely: (*i*) a primordial indigenous source identified in apatites (1–4), volcanic glasses (5, 6), and plagioclase phases (7) supporting a common origin of water for the Earth–Moon system (8–10); (*ii*) an addition of H_2O-rich material via impacts of carbonaceous chondrites (CCs) and cometary materials (11, 12); and (*iii*) a proton implantation by the solar wind (SW) (13–18). Because magmatic water was incorporated in apatites, i.e., in the last minerals crystallized from lunar melts, the D/H ratio of these minerals was used to identify the source of this water. Indeed, all inner solar system objects (Earth, Moon, CCs) show an average water D/H ratio around 150×10^{-6} with variations lying between 125×10^{-6} and 220×10^{-6}. However, in lunar materials, a variety of processes may have altered this D/H ratio, namely: isotopic fractionation during the outgassing of the melt under vacuum, the reduction of water into H_2 by the highly reduced lunar melts, or the contribution of D from spallation reactions. The possible oxidation of SW H into water during silicate melting could also be considered as a possible source for this mantellic water. Indeed, production of water by SW implantation is now considered as a ubiquitous process in the solar system (13, 19) and one of the possible mechanisms for bringing water to the Moon's surface. However, its contribution relative to chondritic or cometary sources is still debated (20).

The D/H ratio (reported here in δD units) is commonly used to identify water sources. However, the Moon being an airless body unprotected by a planetary magnetic field, space weathering (21) modifies the δD of implanted H or of water adsorbed on grains, complicating the identification of the sources. Several types of space contributions can be distinguished: (*i*) water vapor deposition (22) resulting from carbonaceous chondrite or comet impacts; (*ii*) low-energy SW particles (~1 keV/u) that are implanted in silicate grains (23), yielding a 200-nm-thick rim; and (*iii*) high-energy solar (SCR; 0.5–1.0 MeV/u) and galactic (GCR, 0.1–10 GeV/u) cosmic rays that penetrate the rocks down to a few centimeters to a few meters, respectively. These high-energy particles are responsible for the production of cosmogenic D and ^{6}Li via the so-called spallation reactions (24, 25). As a consequence, the D/H ratios of the rim and of the interior of grains do not record the same information: (*i*) The rim contains SW H, cosmogenic elements, and water redeposited after the impacts of water-rich bodies, whereas (*ii*) the interior of grains contains the cosmogenic elements and lunar volatiles trapped in the melt.

To estimate the relative proportions of SW and cosmogenic D in the hydrogen budget of grains in soils, we use the ^{7}Li/^{6}Li ratio as a record of the average concentration of spallation products (26). This approach offers two advantages: (*i*) The amount of cosmogenic D is considered as a free parameter and does not rely on the usual assumptions of theoretical calculations of spallation yields (5, 8, 9, 13), and (*ii*) in addition to a small isotope fractionation restricted to 6‰ (27), departure of the ^{7}Li/^{6}Li ratio toward low values can be unambiguously attributed to the contribution of the cosmogenic ^{6}Li (28) [the cosmogenic ^{7}Li/^{6}Li ratio lies between 1.4 and 2.0 (29) while the lunar ratio is 12.15].

Results

The regolith is the actual boundary between lunar bedrock and interplanetary space. Soil represents the fine fraction <1 mm of the lunar regolith, produced in large part by meteorite impacts with some pyroclastic volcanic contributions. The chemistry and

Significance

The hydrogen isotopic ratio of water is commonly used to identify water sources. However, because the Moon is an airless body, the external fluxes of particles and solids that reach its surface should represent an important contribution to its hydrogen budget and thus alter its pristine D/H ratio. To estimate the relative proportions of the solar wind and of the cosmogenic deuterium in the hydrogen budget, the lithium and the hydrogen isotope ratios were measured simultaneously with the Cameca NanoSIMS 50. Analyses demonstrate that all D comes from spallation reactions. On the surface of the soil grains, their D/H ratios indicate that this source of "water" can be ascribed to solar wind implantation and that the chondritic contribution is negligible.

Author contributions: F.R. designed research; A.S. performed research; A.S. and F.R. analyzed data; and A.S. wrote the paper.

The authors declare no conflict of interest.

This article is a PNAS Direct Submission.

[1]To whom correspondence should be addressed. Email: astephant@mnhn.fr.

This article contains supporting information online at www.pnas.org/lookup/suppl/doi:10.1073/pnas.1408118111/-/DCSupplemental.

mineralogy of the lunar soils reflect the composition of the underlying bedrock. Thus, mare areas have a basaltic composition with high Fe and low Al contents whereas highland areas tend to be more anorthositic in composition, with high Ca and Al values (30). Eighteen different sections from Apollo 16 deep drill core 60007/1, from Apollo 16 double drive tube 60010/9, and from Apollo 17 deep drill core 70009/1 were provided by National Aeronautics and Space Administration (NASA). The Apollo 16 site is located in a highland area whereas the Apollo 17 site is located in an area where highland hills meet the mare plains. We have selected 45 grains representative of the petrography and of the chemical variations in the lunar regolith: agglutinates, volcanic glasses, and plagioclase feldspars. SEM analyses were performed on each grain to identify them. Plagioclases are pristine samples from the primary crust derived from lunar magma ocean crystallization (7) and, because of their highland origin, are keys to constraining the origin of water at the time of the Moon's formation (8). The five plagioclases are closed to the anorthite ($CaAl_2Si_2O_8$) end-member, identified by their high contents in Al and Ca and their depletion in Na. They are all highland-derived components (from Apollo 16 cores). Volcanic glasses are derived from the mare area of Apollo 17 and were identified by their high Mg/Al ratio. Agglutinates are produced by impact gardening and are more inclined to retain space interaction information (13). They show typical irregular shapes. Thus, materials formed by regolith processes and materials derived from highland and mare bedrocks are represented in our sampling. Images and chemistry of the different grains are presented in Fig. 1 (see also Table S1). These cores are samples that illustrate the complexity of the lunar regolith (31–33). Two terrestrial basaltic glasses were used as standards (34).

NanoSIMS measurements were performed both in the rim (<150 nm) and in the interior (1–3 μm depth) of the grains. In the rim, we measured the D^-/H^- and the $^{16}OH^-/^{29}Si^-$ ionic ratios, and in the interior, the D^+/H^+ and the $^7Li^+/^6Li^+$ ratios. Equivalent water concentrations are obtained via an appropriate calibration of the $^{16}OH^-/^{29}Si^-$ ionic ratio. Analytical parameters used for these measurements allow us to rule out any OH contamination

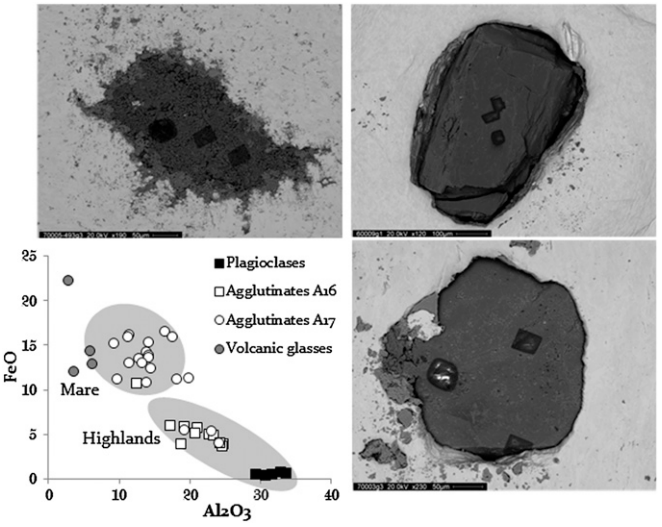

Fig. 1. Image and chemistry of the different grains analyzed in this study: (*i*) agglutinates, (*ii*) anorthite plagioclases, and (*iii*) volcanic glasses. FeO and Al_2O_3 compositions are presented to distinguish the grains derived from highland and those from mare. Circles represent grains of Apollo 17 deep drill core 70009/1; squares represent grains of Apollo 16 double drive tube 60010/9 and Apollo 16 deep drill core 60007/1. Apollo 17 being in a region where the highlands meet the mares, both chemical compositions are present along the core. Plagioclases are found only in Apollo 16, as it is the common mineral in anorthositic rocks.

(35). We use the two basaltic glasses for the calibration of $^{16}OH^-/^{29}Si^-$ versus H_2O/SiO_2 wt %. Calibration was done for each session. Slopes and relative errors were estimated using the R program. Water concentrations are reported as [H_2O] (parts per million) with corresponding errors in Table 1. These concentrations range from 258 ± 2 ppm to 9.60 ± 0.08 wt % H_2O. The D^+/H^+ and the $^7Li^+/^6Li^+$ ionic ratios were converted through calibrations into their corresponding isotopic D/H and $^7Li/^6Li$ ratios reported in Table 1. In the rims, δD values range from −680 ± 3‰ to +7 ± 8‰. In the grain interior, δD values range from −538 ± 17‰ to +3650 ± 169‰ and the δ^7Li from +30 ± 1‰ to −293 ± 0.8‰. No correlation is apparent with any characteristic (chemistry, petrology, depth) of the grains.

Discussion

Spallation Production. Fig. 2 illustrates the expected correlations for the spallation production of D and Li as a function of the Li/H concentration ratio in the interiors of the grain. At the irradiation time *t*, D/H and $^7Li/^6Li$ isotopic ratios can be expressed as an addition of cosmogenic products to the initial ratios:

$$\frac{D}{H}(t) = \frac{D_0 + \phi_D \times t}{H_0} \quad [1]$$

$$\frac{^6Li}{^7Li}(t) = \frac{^6Li_0 + \phi_{6Li} \times t}{^7Li_0} \quad [2]$$

with D_0, H_0, $^6Li_0$, and $^7Li_0$ as the initial concentrations; ϕ_D and ϕ_{6Li} are the spallation production rates of D and ^6Li, respectively.

From the previous equations, we can calculate the equation between the hydrogen and lithium isotopic ratio of the lunar grain at instant *t*:

$$\frac{D}{H}(t) = \frac{\phi_D}{\phi_{6Li}} \times \frac{^7Li_0}{H_0} \times \frac{^6Li}{^7Li}(t) - \frac{\phi_D}{\phi_{6Li}} \times \frac{^6Li_0}{H_0} \times \frac{D_0}{H_0}. \quad [3]$$

Thus, the correlation between D/H(t) and $^6Li/^7Li(t)$, resulting in an addition of cosmogenic products, depends on (*i*) the ratio of initial $^7Li_0/H_0$ concentrations and (*ii*) the production rate ratio. Because of their various chemical compositions—hence their various Li/H ratio—the grains do not lie on a single correlation. It is however possible to calculate, from these isotope ratios, the absolute amount of cosmogenic products.

The amount of cosmogenic ^6Li was calculated as the excess of ^6Li with respect to the lunar $^7Li/^6Li$ ratios as follow:

$$\frac{^7Li_{measured}}{^6Li_{measured}} = \frac{^7Li_{ref}}{^6Li_{ref} + ^6Li_{cosmogenic}}. \quad [4]$$

Similarly, cosmogenic D was calculated for with respect to the lowest measured δD value, i.e., −550‰ for the interior of grains:

$$\frac{D_{measured}}{H_{measured}} = \frac{D_{ref} + D_{cosmogenic}}{H_{ref}}. \quad [5]$$

This is a conservative hypothesis since even lower δD values were reported in the literature (13). Note however that using the theoretical SW value—i.e., δD = −1000‰—has a negligible effect in the calculated cosmogenic D concentration. For the grain rim, no preserved endogenic D is expected. Thus, D measured corresponds to the D produced by spallation. Values are available in Table S2. Fig. 3 *A* and *B* shows the correlations between the cosmogenic D and ^6Li (expressed relative to $^{29}Si^-$) both at the surface and in the interior of grains. Statistical coefficients attest to the significance of these correlations ($R^2 = 0.51$ and 0.65 for Fig. 3 *A* and *B*, respectively). Note that, because the high SW $^7Li/^6Li$ ratio could induce an additional scatter in the calculated cosmogenic ^6Li (26), the Li isotope composition was not measured in the

Table 1. NanoSIMS measurements of Apollo deep drill core 70009/1, Apollo deep drill core 60007/1, and Apollo double drive tube 60010/9

Sample	$D/H_{surface}$, ‰	$^{16}OH^-/^{29}Si^-_{surface}$	$29Si^-$, cps/s	H_2O, ppm	$D/H_{interior}$, ‰	$^7Li/^6Li_{interior}$
			Deep Drill Core 70009/1			
70001.79.3, depth: 280–?						
Grain 1	−312 ± 7	1.15	6,064	3,284 ± 23	828 ± 36	11.17 ± 0.01
Grain 2	−680 ± 3	1.05	26,709	3,124 ± 22	11 ± 49	11.25 ± 0.06
Grain 3	−239 ± 6	1.32	28,727	3,044 ± 21	—	—
70002.470.33, depth: 256.9–257.4						
Grain 1	−240 ± 9	12.04	1,422	33,021 ± 234	−63 ± 29	11.50 ± 0.01
Grain 2	−426 ± 4	4.90	2,653	13,125 ± 93	—	—
Grain 3	−437 ± 4	10.86	6,018	29,075 ± 205	876 ± 49	10.87 ± 0.01
70003.547.41, depth: 218.7–219.2						
Grain 1	−307 ± 5	2.41 ± 0.22	5,997	6,460 ± 587	−293 ± 29	9.35 ± 0.01
Grain 2	−232 ± 5	3.45 ± 0.64	4,351	8,854 ± 1654	1,019 ± 40	8.91 ± 0.01
70004.582.47, depth: 180.2–180.7						
Grain 2	−530 ± 4	0.93	5,845	2,537 ± 18	—	—
Grain 3	−618 ± 6	0.57	59,120	1,454 ± 10	—	—
70005.494.84, depth: 158.8–159.3						
Grain 1	−289 ± 4	3.10	11,171	8,566 ± 60	231 ± 51	9.79 ± 0.02
Grain 2	−254 ± 4	3.05	14,550	8,017 ± 57	3,650 ± 169	11.27 ± 0.01
70005.493.177, depth: 134.8–135.3						
Grain 1	—	1.10	—	2,702 ± 19	147 ± 48	9.39 ± 0.02
Grain 2	−412 ± 5	1.06	1,032	2,739 ± 20	989 ± 91	9.11 ± 0.01
Grain 3	−241 ± 6	0.99	46,395	2,623 ± 18	554 ± 44	8.99 ± 0.01
70006.514.36, depth: 98.4–98.8						
Grain 2	−518 ± 4	0.61	72,993	1,875 ± 15	154 ± 7	12.41
Grain 3	−43 ± 18	0.66	33,473	2,053 ± 17	−538 ± 17	11.48 ± 0.04
70007.460.146, depth: 73.9–74.4						
Grain 1	7 ± 8	0.43	43,528	1,337 ± 11	178 ± 11	12.39
Grain 2	−237 ± 7	0.63	52,130	1,934 ± 16	1,728 ± 19	12.42
Grain 3	−228 ± 7	0.79	48,532	2,444 ± 20	781 ± 13	12.17
70008.528.160, depth: 28.4–28.8						
Grain 1	−31 ± 10	0.51	57,545	1,571 ± 13	1,029 ± 37	12.48 ± 0.01
Grain 2	−205 ± 9	0.96	48,417	2,967 ± 24	2,123 ± 35	12.81 ± 0.01
Grain 3	−196 ± 9	0.50	37,968	1,536 ± 12	2,181 ± 31	11.72
70009.560.11, depth: 16.0–16.5						
Grain 1	−501 ± 10	0.60	21,654	1,851 ± 15	−405 ± 25	11.21 ± 0.03
Grain 2	−462 ± 6	0.39	86,198	1,206 ± 10	645 ± 41	12.99 ± 0.01
Grain 3	−400 ± 7	0.36	32,478	1,102 ± 9	1,142 ± 29	11.95 ± 0.01
			Deep Drill Core 60007/1			
60004.670.269, depth: 120.2–120.7						
Grain 1	−303 ± 4	0.47	23,560	1,447 ± 11	354 ± 10	11.19
Grain 2	−187 ± 6	0.42	24,020	1,364 ± 11	733 ± 32	11.14 ± 0.01
Grain 3	−93 ± 13	0.46	10,145	1,337 ± 10	—	—
60006.419.131, depth: 22.9–23.7						
Grain 1	−365 ± 10	0.81	19,855	2,176 ± 17	—	—
Grain 2	−72 ± 17	1.17	9,004	3,737 ± 29	—	—
Grain 3	−300 ± 7	1.30	15,897	3,838 ± 30	2,131 ± 207	12.51 ± 0.03
Grain 4	−209 ± 7	0.64	50,442	1,896 ± 15	1,572 ± 25	12.06 ± 0.01
60007.518.90, depth: 17.6–18.1						
Grain 1	−30 ± 7	1.69	897	5,249 ± 41	719 ± 48	9.03 ± 0.02
Grain 2	−121 ± 6	0.61	49,427	1,946 ± 15	—	—
Grain 3	−257 ± 5	0.79	16,145	2,313 ± 18	—	—
			Double Drive Tube 60010/9			
60009.1272. 1130, depth: 53.5–54.0						
Grain 1	542 ± 33	0.09	5,607	258 ± 2	1,277 ± 40	11.82 ± 0.02
Grain 2	−155 ± 20	0.37	9,712	1,187 ± 9	2,064 ± 36	11.62 ± 0.01
Grain 3	−213 ± 13	0.34	12,363	1,167 ± 9	−28	12.42 ± 0.01
60010.3241.3027, depth: 20.0–20.5						
Grain 1	−293 ± 6	1.35	29,739	13,127 ± 24	665 ± 20	11.67 ± 0.01
Grain 2	−490 ± 6	18.02 ± 0.01	2,908	49,921 ± 388	1,368 ± 17	12.34
Grain 3	−252 ± 8	36.59 ± 0.02	1,667	96,508 ± 750	−290 ± 20	10.57 ± 0.02
60010.482.176, depth: 0.5–1.0						
Grain 1	−146 ± 6	0.48	21,537	1,399 ± 11	167 ± 49	10.91 ± 0.03
Grain 2	−188 ± 7	0.99	4,129	2,967 ± 23	—	—
Grain 3	−312 ± 6	0.62	43,595	1,807 ± 14	3,639 ± 138	10.77 ± 0.01

D/H and $^7Li/^6Li$ ratios are corrected from the IMS fractionation. OH^-/Si^- ratios that don't have uncertainties mean that uncertainties are lower than 0.01 and so can be considered as negligible.

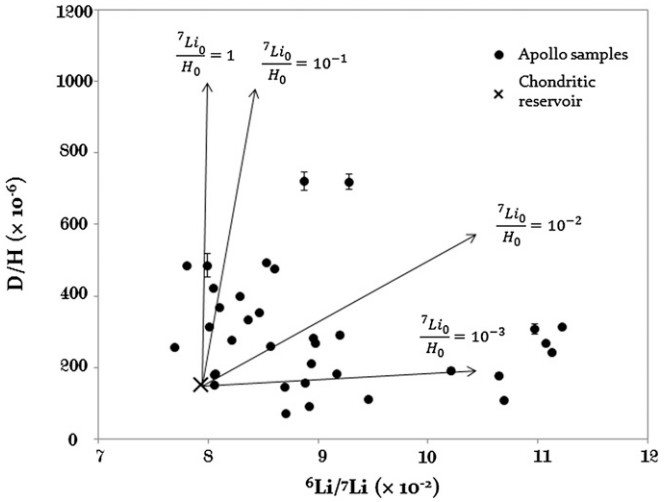

Fig. 2. D/H versus $^6Li/^7Li$ at the interior of grains of Apollo 60010/9, 60007/1, and 70009/1 samples. Theoretical correlations between D/H and $^6Li/^7Li$ by simple addition of cosmogenic products are drawn using Eq. **3** and for various $^7Li_0/H_0$ (i.e., 1, 10^{-1}, 10^{-2} and 10^{--}), starting from a chondritic reservoir. The aim of this diagram is to show that the Li and H isotope ratios are not expected to be correlated if spallation took place on grains of different initial chemical compositions. Note also that some grains exhibit a D/H ratio bellow the chondritic value, suggesting that the lunar H is < 8 x10^{-5}.

rim. Moreover, the theoretical production rate ratio of D/^{6}Li is drawn as lines in Fig. 3 *A* and *B*, using the ratio of their cross sections [σ_D = 11 mbarn (mb) from Merlivat et al. (25) and σ_{6Li} = 15 mb from Chaussidon and Robert (26) and Reeves (36) for energy >0.1 GeV/u, i.e., for GCR], reinforcing the interpretation according to which the calculated excesses of D and ^{6}Li have a cosmogenic origin. In addition, none of the grains from mare basalt or highland areas, glassy or well-crystallized plagioclases, whatever their provenance or depth, depart from these correlations. However, a possible contribution of an indigenous lunar H having an isotopic composition lower than the lowest measured value cannot be excluded; that is $\delta D \leq -550‰$.

Exposure to the Solar Wind at the Moon Surface. On the Moon, exposure ages cover a wide range, from material lying near the surface for a billion years to material never exposed to cosmic

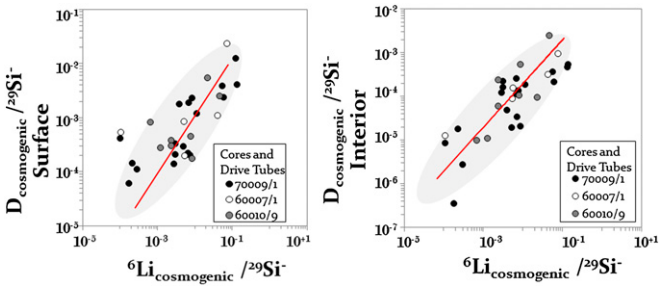

Fig. 3. $D_{Cosmogenic}/^{29}Si^-$ versus $^6Li_{Cosmogenic}/^{29}Si^-$ (*A*) at the surface and (*B*) in the interior of grains of Apollo 60010/9, 60007/1, and 70009/1 samples. Cosmogenic ^{6}Li is the excess produced by spallation calculated relative to lunar value (12.15). $D_{Cosmogenic}$ is the excess relative to the lowest value measured in the interior of grains ($\delta D = -550‰$, i.e., D/H = 70 x 10^{-6}) and to all D, for the surface. Red lines correspond to the theoretical spallation production rate ratio $D_{Cosmogenic}/^6Li_{Cosmogenic}$. The correlations of $D_{Cosmogenic}/^{29}Si^-$ vs. $^6Li_{Cosmogenic}/^{29}Si^-$ and their agreement with the theoretical $D_{Cosmogenic}/^6Li_{Cosmogenic}$ ratio indicate that almost all of the D is of cosmogenic origin. At the surface of the grains, the scattering of the data may be attributed to a chondritic contribution of H, but restricted to 15% of the bulk H.

rays. Exposure ages of sections from deep drill cores and double drive tubes were reviewed by Meyer (31–33). Based on available literature data (*Materials and Methods*), we have identified that the 70006, 70007, 70008, 60004, and 60009 levels in the cores were never exposed to the lunar surface, i.e., to the SW. Using this criterion, a plot of δD vs. H_2O content (parts per million) on rims of these two categories of grains, i.e., exposed and not exposed to the Moon's surface, is drawn in Fig. 4. Exposed grains exhibit systematically higher H_2O content up to 9.60 ± 0.08 wt % H_2O and lower D/H ratios as low as −680 ± 3‰ (i.e., closer to the SW value; −1,000‰), indicating again that "water" in lunar soils is essentially of solar origin. Moreover, mixing lines between spallation and chondritic or solar wind end members are drawn to highlight the mixing of these three sources. Since most data plots below the chondritic correlation, the chondritic contribution to the lunar indigenous H is negligible. A similar conclusion was reached to account for the widespread OH spectra observed by Chandrayyan-1 IR spectrometer on the lunar surface (14, 17). Furthermore, the production of hydroxyl groups (OH) in basalt by H implantation of SW-type protons was reproduced experimentally on lunar analogs (37) and lunar soils (38). This is also in agreement with the study of Liu et al. (13).

Estimation of the Chondritic Contribution. However, because of the scattering of the data around the theoretical ^{6}Li/D production rate ratio, a possible chondritic contribution in the rim of exposed grains is measurable. Assuming that the D excess relative to the cosmogenic correlation line reported in Fig. 3*A* is due to a contribution of chondritic water having a D/H ratio of 150×10^{-6}, the corresponding H content can be estimated and converted into a percentage of the total amount of H in the grains.

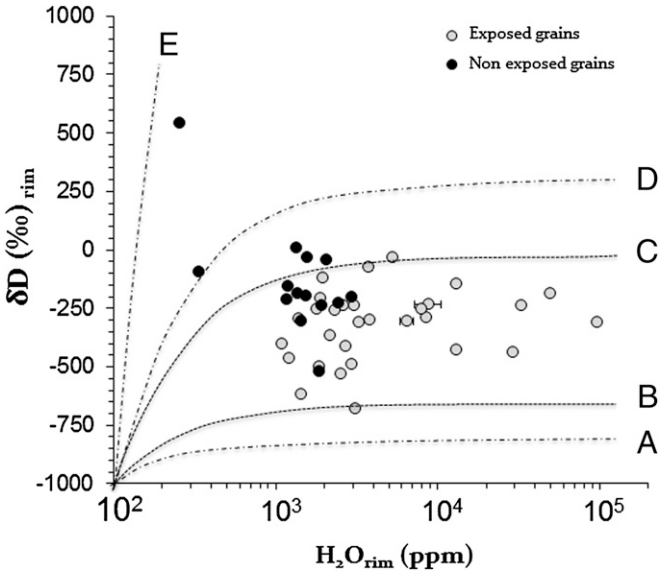

Fig. 4. δD versus H_2O content (parts per million) in the rim of the grains (thickness 150 nm). Two sets of data are distinguished according to their degree of exposure to the SW: "exposed" as open symbols and "nonexposed" as black symbols. The nonexposed sections are 60004,670,269; 60009,1172,1130; 70006,514,36; 70007,460,146; and 70008,528,160. The continuous addition of cosmogenic D and SW H (curves a, d, and e) to a SW end member (−1000‰; 100 ppm H_2O) is shown for a relative spallation contribution of 1/10, ½, and 2/1 for curves a, d, and e, respectively. An additional chondritic contribution to curves a and d (with 1/5 the chondritic/SW ratio) is shown by curves b and c. The aim of the figure is to show that the respective relative contributions of cosmogenic and chondritic D cannot be determined in a H versus D/H diagram. Using the cosmogenic ^{6}Li, it is presently calculated that the cosmogenic D stands for the dominant contribution. Accordingly, SW H is the dominant source of H (expressed as H_2O) on the grain rims.

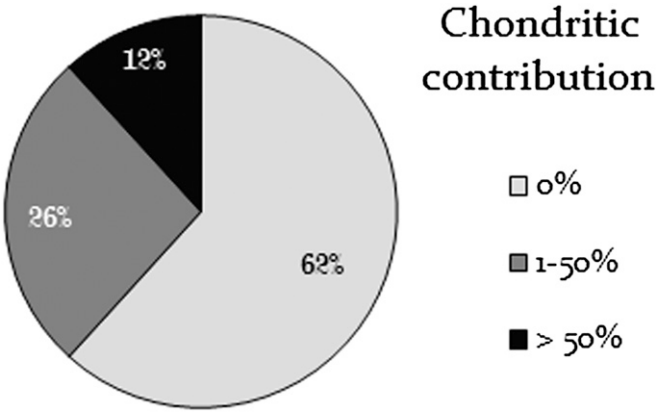

Fig. 5. Chondritic contribution onto the rim of Apollo soil grains. Diagram showing the maximum possible chondritic contribution on the surface of 34 grains isolated at different depth from three lunar cores. H chondritic contributions range from 0% to 83%.

Thus, it can be calculated that 62% of grains are essentially free of this chondritic contribution (Fig. 5). The others grains would exhibit a chondritic contribution ranging from 3% to 83% (Table S2), corresponding to a maximum water concentration of 5 wt % H_2O. Considering the percentage of H chondritic contribution for each grain, the mean value for this contribution is 15%, meaning that the soil may contain an average of 15% of hydrogen from chondritic water. Such an average concentration is much lower than expected if all of the water brought by comets or carbonaceous chondrites over one billion years were deposited in the soils. These estimates must be regarded as maximum upper limits because we have ignored the possible H loss in space due to the sputtering of the grains by the SW.

To summarize the conclusions of this study on soil grains: (*i*) hydroxyl groups are mostly due to SW implantation, (*ii*) water vapor arising from CCs or comet impacts is not efficiently trapped in grain rims, and (*iii*) no detectable amounts of a chondritic hydrogen is retained inside grains.

Materials and Methods

Samples. Two terrestrial basaltic glasses DR15-2-5 and DR20-1-1 from the Southern Indian Ridge (SWIR) were used for instrumental mass fractionation and water concentration calibration. Chemical compositions are given in Table S3 (34). Samples were mounted to reduce the contribution of epoxy to the OH signal: Holes were drilled in a 10-mm aluminum disk with a 2-mm-diameter drill bit. In each hole, samples were mounted individually with epoxy and then polished successively with 1-μm and 0.25-μm diamond paste to produce a planar surface. The mount was then cleaned in an ultrasonic bath of ethanol and then carbon-coated, thickness 20 nm. Lunar grains were pressed into indium foil to avoid any terrestrial contamination and to preserve both their rim and interior.

Apollo 16 deep drill core 60007/1. Core 60007/1 sampled ~2 m of regolith from the Cayley Plains. Four major stratigraphic units were distinguished along this core from compositions and modal abundances of clast sizes (24, 32). Based on maturity of soils with ferromagnetic resonance studies (i.e., Is/FeO), Gose and Morris (39) suggested that the first unit A was never exposed to the surface and the three other units below 13 cm (B, C, and D) were deposed in a single impact event and subjected to reworking during 450 million years. The last 13 cm were added 50 million years ago. This is also in agreement with noble gas data of Bogard and Hirsch (40). From data of Gose and Morris (39), we notice that section 60004,670,269 is a submature soil whereas 60006,419,131 and 60007,518,90 are mature soils. Thus, 60004,670,269, being at ~120.5 cm depth, can be considered as never exposed at the Moon surface, unlike the others samples.

Apollo 16 double drive tube 60010/9. Tube 60010/9 sampled ~60 cm of regolith. From ferromagnetic resonance studies (41), 60009,1172,1130 was determined as an immature/submature soil whereas 60010,3241,3027 and 60010,482,176 increase in maturity, with submature and mature features, respectively. They considered a single deposition of the core 100 million years ago and in situ reworking of the top 12,5 cm. Sample 60010,482,176 was sampled in the top centimeters (0.5–1 cm) and thus had undergone in situ reworking for 125 million years, constrained by cosmogenetic ^{21}Ne measurements (42) and its higher maturity index. Blanford et al. (43) highlighted the presence of a buried soil surface at 50–52 cm by track measurements. Section 60009,1172,1130 is located below the ancient lunar surface, in a soil unit undisturbed where the track density frequency distribution does not have the characteristic of surface soils and can be considered as a soil not exposed to lunar surface.

Apollo 17 deep drill core 70009/1. Core 70009/1 is the longest core recovered (~3 m) and has the longest depositional history. According to Nagle (44), the story of the core is likely as follows: Between 210 cm and 275 cm, an ancient avalanche deposited highly irradiated soil (70002,470,33 and 70003,547,41) on the basalt-rich zone below 275 cm, which is the oldest valley floor surface (70001,79,3). The surface of the avalanche deposit was gardened between time of deposition (1.5–1.6 billion years ago) and ~100 million years, when secondary impacts from Tycho deposited unirradiated basalt fragments from 111 cm to the surface. It is in agreement with analyses of Crozaz and Ross (45), who identified an intermediate layer from 20 cm to 60 cm of soils with very low irradiation and thus never exposed to the lunar surface. From this information, 70006,514,36, 70007,460,146, and 70008,528,160 are classified as nonexposed soils. The upper 20 cm shows a high level of irradiation, characteristic of a reworking zone (70009,560,11).

From these depositional histories of the three cores, we separate the five sections, defined as nonexposed to the lunar surface and not irradiated by solar wind (60004,670,269; 60009,1172,1130; 70006,514,36; 70007,460,146; and 70008,528,160), from other sections in order to compare their rim δD (‰) and $^{16}OH^-/^{29}Si^-$ ratio, which is relative to the water concentration.

NanoSIMS Measurements. Analyses were performed with the Cameca NanoSIMS 50 at the Museum National d'Histoire Naturelle, Paris. On each grain, two analyses were achieved. At the grain surface (<150 nm depth), elemental (^{13}C, ^{16}OH, ^{29}Si) and isotopic hydrogen (H, D) compositions were imaged using a 16-keV cesium primary ion beam of 200 pA. Analyses were performed on a 20 × 20 μm^2 surface area, 256 × 256 pixels after a presputtering of 20 min on a 25 × 25 μm^2 surface area with same intensity of the primary beam. Inside grains (2–3 μm depth), hydrogen and lithium isotopic measurements were imaged simultaneously using an oxygen primary beam of 30 nA on a 20 × 20 μm^2 surface area, 256 × 256 pixels. The switch from cesium to oxygen source was required to combine both exterior and interior grain measurements. A presputtering of 2 min was done before each analysis. Depths of analyses were measured with an atomic force microscope at Université de Lille, France. Samples were introduced 1 wk before analysis in the airlock in order to let them outgas. The vacuum in the analysis chamber was also below 1 × 10^{-9} torr. Three different sessions of measurements were necessary for the three Apollo cores, and each set of data was corrected for instrumental mass spectrometer fractionation with analyses made on standards during each session. Data were processed with the L'IMAGE software developed by L. Nittler (46). The dead time was set at 44 ns, and the corresponding correction is included in the L'IMAGE software.

ACKNOWLEDGMENTS. A.S. thanks B. Laurent for atomic force microscope measurements, R. Duhamel and A. Gonzales for assistance during NanoSIMS analyses, and L. Remusat for helpful discussions. We thank R. Hewins for helpful corrections. We also thank Pierre Cartigny for providing basaltic glass standards. We gratefully acknowledge NASA for providing samples. The National NanoSIMS facility at the Muséum National d'Histoire Naturelle was established by funds from Centre National de la Recherche Scientifique, Région Île de France, Ministère délégué à l'Enseignement supérieur et à la Recherche, and the museum itself.

1. Boyce JW, et al. (2010) Lunar apatite with terrestrial volatile abundances. *Nature* 466(7305):466–469.
2. McCubbin FM, et al. (2010) Nominally hydrous magmatism on the Moon. *Proc Natl Acad Sci USA* 107(25):11223–11228.
3. Barnes JJ, et al. (2013) Accurate and precise measurements of the D/H ratio and hydroxyl content in lunar apatites using NanoSIMS. *Chem Geol* 337-338:48–55.
4. Tartèse R, et al. (2013) The abundance, distribution, and isotopic composition of hydrogen in the Moon as revealed by basaltic lunar samples: Implications for the volatile inventory of the Moon. *Geochim Cosmochim Acta* 122:58–74.
5. Füri E, Deloule E, Gurenko A, Marty B (2014) New evidence for chondritic lunar water from combined D/H and noble gas analyses of single Apollo 17 volcanic glasses. *Icarus* 229:109–120.

6. Saal AE, et al. (2008) Volatile content of lunar volcanic glasses and the presence of water in the Moon's interior. *Nature* 454(7201):192–195.
7. Hui H, Peslier AH, Zhang Y, Neal CR (2013) Water in lunar anorthosites and evidence for a wet early Moon. *Nat Geosci* 6(3):177–180.
8. Barnes JJ, et al. (2014) The origin of water in the primitive Moon as revealed by the lunar highlands samples. *Earth Planet Sci Lett* 390:244–252.
9. Saal AE, Hauri EH, Van Orman JA, Rutherford MJ (2013) Hydrogen isotopes in lunar volcanic glasses and melt inclusions reveal a carbonaceous chondrite heritage. *Science* 340(6138):1317–1320.
10. Tartèse R, et al. (2014) Apatites in lunar KREEP basalts: The missing link to understanding the H isotope systematics of the Moon. *Geology* 42(4):363–366.
11. Greenwood JP, et al. (2011) Hydrogen isotope ratios in lunar rocks indicate delivery of cometary water to the Moon. *Nat Geosci* 4(2):79–82.
12. Elkins-Tanton LT, Grove TL (2011) Water (hydrogen) in the lunar mantle: Results from petrology and magma ocean modeling. *Earth Planet Sci Lett* 307(1-2):173–179.
13. Liu Y, et al. (2012) Direct measurement of hydroxyl in the lunar regolith and the origin of lunar surface water. *Nat Geosci* 5(11):779–782.
14. McCord TB, et al. (2011) Sources and physical processes responsible for OH/H_2O in the lunar soil as revealed by the Moon Mineralogy Mapper (M3). *J Geophys Res* 116(E6): E00G05.
15. Clark RN (2009) Detection of adsorbed water and hydroxyl on the Moon. *Science* 326(5952):562–564.
16. Füri E, Marty B, Assonov SS (2012) Constraints on the flux of meteoritic and cometary water on the Moon from volatile element (N-Ar) analyses of single lunar soil grains, Luna 24 core. *Icarus* 218(1):220–229.
17. Pieters CM, et al. (2009) Character and spatial distribution of OH/H_2O on the surface of the Moon seen by M3 on Chandrayaan-1. *Science* 326(5952):568–572.
18. Sunshine JM, et al. (2009) Temporal and spatial variability of lunar hydration as observed by the Deep Impact spacecraft. *Science* 326(5952):565–568.
19. Bradley JP, et al. (2014) Detection of solar wind-produced water in irradiated rims on silicate minerals. *Proc Natl Acad Sci USA* 111(5):1732–1735.
20. Burke DJ, et al. (2011) Solar wind contribution to surficial lunar water: Laboratory investigations. *Icarus* 211(2):1082–1088.
21. Lucey P, et al. (2006) Understanding the lunar surface and space-Moon interactions. *Rev Mineral Geochem* 60(1):83–219.
22. Noble SK, Keller LP, Pieters CM (2005) Evidence of space weathering in regolith breccias I: Lunar regolith breccias. *Meteorit Planet Sci* 40(3):397–408.
23. Keller LP, McKay DS (1997) The nature and origin of rims on lunar soil grains. *Geochim Cosmochim Acta* 61(11):2331–2341.
24. Vaniman DT, Reedy R, Heiken G, Olhoeft G, Mendell W (1991) The lunar environment. *Lunar Sourcebook: A User's Guide to the Moon*, eds Heiken GH, Vaniman DT, French BM (Cambridge Univ Press, Cambridge, UK), pp 27–60.
25. Merlivat L, Lelu M, Nief G, Roth E (1976) Spallation deuterium in rock 70215. *Proc Lunar Planet Sci Conf* 7:649–658.
26. Chaussidon M, Robert F (1999) Lithium nucleosynthesis in the Sun inferred from the solar-wind 7Li/6Li ratio. *Nature* 402(6759):270–273.
27. Seitz H-M, et al. (2006) Lithium isotope compositions of Martian and lunar reservoirs. *Earth Planet Sci Lett* 245(1-2):6–18.
28. Vangioni-Flam E, et al. (1999) Lithium-6: Evolution from Big Bang to present. *New Astron* 4(4):245–254.
29. Reeves H (1993) On the origin of the light elements (Z<6). *Origin and Evolution of the Elements*, eds Prantzos N, Vangioni-Flam E, Cassé M (Cambridge Univ Press, Cambridge, UK), pp 168–197.
30. Lindsay JF (1976) The lunar soils. *Lunar Stratigraphy and Sedimentoly*, eds Kopal Z, Cameron AGW (Elsevier, Amsterdam), pp 227–285.
31. Meyer C (2007) *Lunar Sample Compendium: 60009-60010* (Natl Aeronaut Space Admin, Greenbelt, MD).
32. Meyer C (2007) *Lunar Sample Compendium: 60007-60001* (Natl Aeronaut Space Admin, Greenbelt, MD).
33. Meyer C (2007) *Lunar Sample Compendium: 70009-70001* (Natl Aeronaut Space Admin, Greenbelt, MD).
34. Clog M (2010) Concentration et composition isotopique de l'hydrogène dans le manteau terrestre. Doctoral thesis (Univ Paris Diderot, Paris).
35. Stephant A, Remusat L, Thomen A, Robert F (2014) Reduction of OH contamination in quantification of water contents using NanoSIMS imaging. *Chem Geol* 380:20–26.
36. Reeves H (2001) The origin of the light elements in the early Universe. *The Century of Space Science*, eds Bleeker JM, Geiss J (Springer, New York), pp 423–440.
37. Managadze GG, Cherepin VT, Shkuratov YG, Kolesnik VN, Chumikov AE (2011) Simulating OH/H_2O formation by solar wind at the lunar surface. *Icarus* 215(1): 449–451.
38. Ichimura AS, Zent AP, Quinn RC, Sanchez MR, Taylor LA (2012) Hydroxyl (OH) production on airless planetary bodies: Evidence from H+/D+ ion-beam experiments. *Earth Planet Sci Lett* 345-348:90–94.
39. Gose WA, Morris RV (1977) Depositional history of the Apollo 16 deep drill core. *Proc Lunar Sci Conf* 8:2909–2928.
40. BogardDDHirschWC (1975) Noble gas studies on grain size separates of Apollo 15 and 16 deep drill cores. *Proc Lunar Sci Conf* 6:2057–2083.
41. Morris RV, Gose WA (1976) Ferromagnetic resonance and magnetic studies of cores 60009/10 and 60003: Compositional and surface exposure stratigraphy. *Proc Lunar Sci Conf* 7:1–11.
42. BogardDDHirschWC (1977) Noble gas evidence for the depositional and irradiational history of 60010-60009 core soils. *Proc Lunar Sci Conf* 8:2983–2999.
43. Blanford GE, Blanford J, Hawkins JA (1979) Irradiation stratigraphy and depositional history of the Apollo 16 double drive tube 60009/10. *Proc Lunar Sci Conf* 10:1333–1349.
44. Nagle JS (1981) An ancient avalanche deposit in the Taurus-Littrow Valley is part of the long depositional history of the Apollo 17 drill core. *Proc Lunar Planet Sci Conf* 12B:519–528.
45. Crozaz G, Ross LM, Jr (1979) Deposition and irradiation of the Apollo 17 deep drill core. *Proc Lunar Sci Conf* 10:1229–1241.
46. Nittler LR, Alexander CMOD (2003) Automated isotopic measurements of micron-sized dust: Application to meteoritic presolar silicon carbide. *Geochim Cosmochim Acta* 67(24): 4961–4980.